



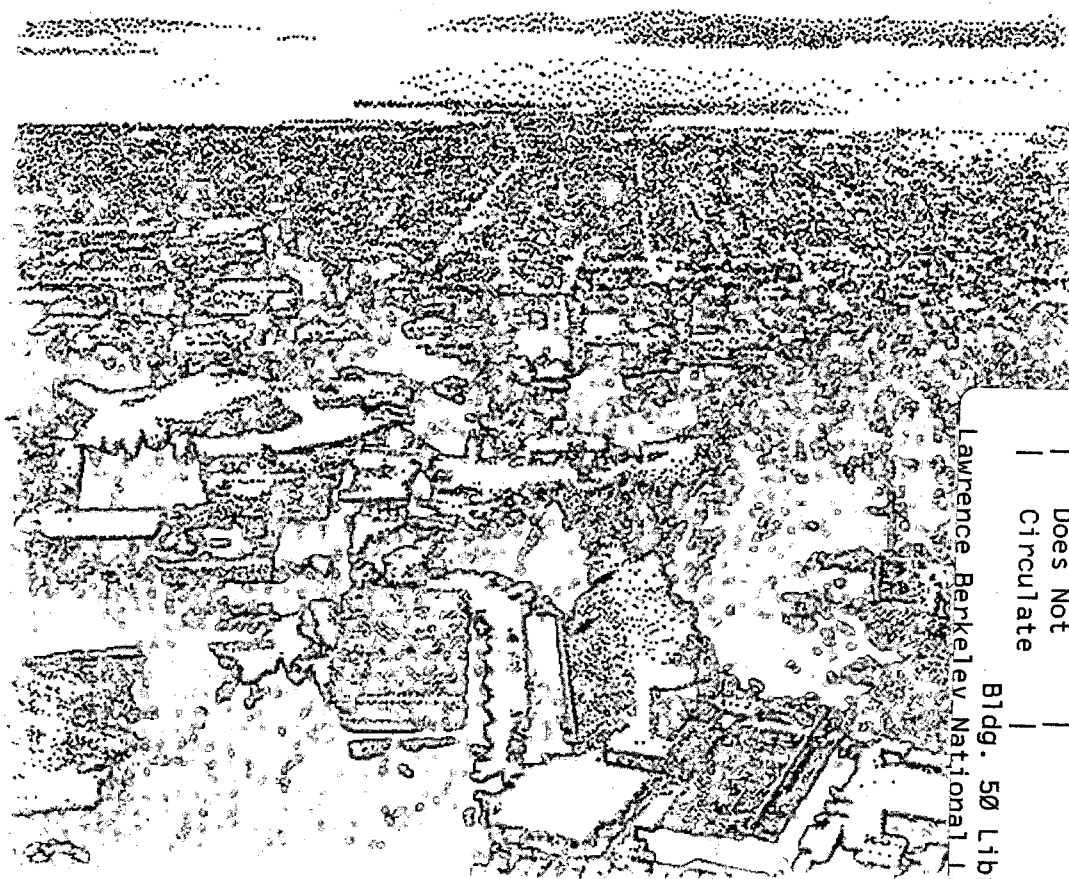
# ERNEST ORLANDO LAWRENCE BERKELEY NATIONAL LABORATORY

## The Shadow of a Conical Intersection

Musahid Ahmed, Darcy S. Peterka,  
and Arthur G. Suits

**Chemical Sciences Division**

May 1997  
Submitted to  
*Science*



Lawrence Berkeley National Laboratory

Bldg. 50 Library - Ref.

REFERENCE COPY |  
Does Not |  
Circulate |

Copy 1

LBNL-40310

#### **DISCLAIMER**

This document was prepared as an account of work sponsored by the United States Government. While this document is believed to contain correct information, neither the United States Government nor any agency thereof, nor The Regents of the University of California, nor any of their employees, makes any warranty, express or implied, or assumes any legal responsibility for the accuracy, completeness, or usefulness of any information, apparatus, product, or process disclosed, or represents that its use would not infringe privately owned rights. Reference herein to any specific commercial product, process, or service by its trade name, trademark, manufacturer, or otherwise, does not necessarily constitute or imply its endorsement, recommendation, or favoring by the United States Government or any agency thereof, or The Regents of the University of California. The views and opinions of authors expressed herein do not necessarily state or reflect those of the United States Government or any agency thereof, or The Regents of the University of California.

Ernest Orlando Lawrence Berkeley National Laboratory  
is an equal opportunity employer.

## **DISCLAIMER**

This document was prepared as an account of work sponsored by the United States Government. While this document is believed to contain correct information, neither the United States Government nor any agency thereof, nor the Regents of the University of California, nor any of their employees, makes any warranty, express or implied, or assumes any legal responsibility for the accuracy, completeness, or usefulness of any information, apparatus, product, or process disclosed, or represents that its use would not infringe privately owned rights. Reference herein to any specific commercial product, process, or service by its trade name, trademark, manufacturer, or otherwise, does not necessarily constitute or imply its endorsement, recommendation, or favoring by the United States Government or any agency thereof, or the Regents of the University of California. The views and opinions of authors expressed herein do not necessarily state or reflect those of the United States Government or any agency thereof or the Regents of the University of California.

LBNL-40310  
UC-401

## **The Shadow of a Conical Intersection**

Musahid Ahmed, Darcy S. Peterka, and Arthur G. Suits

Chemical Sciences Division  
Ernest Orlando Lawrence Berkeley National Laboratory  
University of California  
Berkeley, California 94720

May 1997

This work was supported by the Director, Office of Energy Research, Office of Basic Energy Sciences, Chemical Sciences Division, of the U.S. Department of Energy under Contract No. DE-AC03-76SF00098.



# The shadow of a conical intersection

Musahid Ahmed, Darcy S. Peterka and Arthur G. Suits\*

*Chemical Dynamics Group*

*Chemical Sciences Division*

*Ernest Orlando Lawrence Berkeley National Laboratory*

*Berkeley, CA 94720*

## Abstract

The technique of velocity map imaging has been applied to the reaction  $O(^1D)+D_2 \rightarrow D+OD$  under single collision conditions in counterpropagating molecular beams at a collision energy of 6.1 kcal/mol. Images of the reactively scattered D atom product were recorded, yielding the full double differential cross sections (energy and angle) for the reaction. The observed D atom angular distribution is strongly peaked  $160^\circ$  from the incoming  $D_2$  beam, showing the importance of abstraction via near collinear geometries. The absence of rebound scattering at  $180^\circ$  is a direct consequence of the conical intersection between the  $1^1A'$  and  $2^1A'$  ( $^1\Sigma^+ + ^1\Pi$ ) surfaces, for which the interaction vanishes in the strictly collinear configuration. The observed scattering distribution is a mapping of the likelihood of abstraction on the ground state potential energy surface onto the accessibility to the product space determined by the conical intersection itself. The absence of directly backscattered reaction flux thus represents the actual shadow of the conical intersection.

---

\*author to whom correspondence should be addressed

Conical intersections between electronic potential energy surfaces in polyatomic molecules arise, for example, when states of different symmetry species are degenerate for a limiting nuclear geometry, but this symmetry is reduced as the geometry is changed [1]. States of different symmetry species do not interact, so that the potential surfaces cross in the limiting geometry. As the geometry is changed the states then interact and repel each other. In the region of the intersection, the Born-Oppenheimer approximation, which assumes separability of electronic and nuclear motion, breaks down. Nonadiabatic 'surface hopping' may then occur, sometimes leading to chemical reaction, sometimes not: these can thus be regions of considerable chemical significance [2,3]. Conical intersections are associated with other extraordinary effects, such as Jahn-Teller and Renner-Teller interactions [1] and the geometric phase [4,5]; they often account for unusual dynamics in photochemical processes [6], and they play a role in some critical biochemical events such as the process of vision and the synthesis of vitamin D [2]. However, experimentally their signature is usually seen indirectly in product state distributions or in spectroscopic perturbations. Their consequences in reaction dynamics, though widely discussed recently [7-11] have rarely been observed directly. Here we present reactive scattering results for an important chemical system, the reaction of  $O(^1D)$  with  $D_2$ , showing dramatic evidence of the role of the conical intersection; the results allow us to explore the relative importance of a ground and excited state contributions to the reaction dynamics at moderate collision energies.

The reaction of  $O(^1D)$  with molecular hydrogen and its isotopic variants has long been considered a prototypical insertion reaction, with most collisions at thermal energies believed to access the region of the deep  $H_2O$ . An early crossed-beam study found forward-backward symmetry in the angular distribution for collision at 2.7 kcal/mol [12]. This was ascribed to an insertion reaction mechanism, with symmetry in the decaying intermediate invoked to account for the angular distribution. Trajectory calculations have consistently shown forward-backward symmetric angular distributions and the importance of the insertion mechanism [13-17] but recent work, both experimental [18-22], and theoretical [16,23,24] has begun to challenge the notion of simple insertion on the ground electronic potential energy surface.

Kuntz et al. were the first to explore the role of excited states in this reaction [23]. They performed a multisurface quasiclassical trajectory (QCT) study of the dynamics of this reaction using the diatomics-in-molecules approach to generate the excited surface. On the ground state surface they found the insertion mechanism dominant, but trajectories run on the first excited surface showed marked dominance of backward scattering with a strong dependence on collision energy, indicating that a rebound abstraction mechanism comes into play with the inclusion of the first excited state surface. However, their 5 kcal/mol barrier to this collinear approach implied a minimal importance for this mechanism under thermal conditions. Liu and coworkers have recently observed enhanced backscattering at 4.55 kcal/mol collision of  $O(^1D)$  with HD; in addition, recent integral cross section measurements from the same laboratory show a minimum around 2 kcal/mol, with a steady increase to higher collision energies. Cassavechia and coworkers have recently observed forward scattering at very low collision energy reaction of  $O(^1D)$  with  $H_2$  [22], also observed recently in our laboratory for reaction with  $D_2$ .

Schatz et al. have developed a global potential surface for the first excited ( $1A''$ ) surface of  $H_2O$ , which they have incorporated in extensive QCT calculations [24]. Their results showed a growing contribution for excited state reaction at energies above the barrier. Based on these theoretical calculations and the recent molecular beam studies, it is now clear that excited electronic states must play some role in this reaction at collision energies above about 2 kcal/mol.

We have begun an in-depth experimental study to explore the role of excited states and nonadiabatic dynamics in this reaction, using the ion imaging technique in counter-propagating and crossed molecular beams. Ion imaging is a multiplexing method providing simultaneous detection of all recoil velocities, both speed and angle, for the detected product [25–27]. One of the most appealing features of the imaging technique is the very direct way the raw data presents itself to the experimenter. Further, the images may be directly deconvoluted to yield the velocity-flux contour maps which summarize the dynamics. The deconvolution does not require the simplifying assumption of uncoupled translational energy

and angular distributions often employed in analyzing reactive scattering experiments. The imaging experiments thus directly reveal the genuine double differential cross sections, a particularly important feature in the  $O(^1D) + D_2$  reaction.

The experiment [28] consists of two counterpropagating pulsed beams, one containing  $O(^1D)$  seeded in helium, the other neat  $D_2$ . Shortly after the beams interact, the product D atoms are ionized by 1+1 resonant photoionization on the axis of a TOF mass spectrometer. The product ions are accelerated onto an imaging detector viewed by a CCD camera, with the detector gated to respond only to the D atom mass. In the past, the ion imaging technique has suffered from limited velocity and angular resolution, determined by the dimensions of the interaction region relative to the detector, and by blurring from lensing effects associated with the grids. A recent advance by Eppink and Parker involves simply replacing the conventional grids of the Wiley-McLaren TOF spectrometer with electrostatic lenses and adjusting the potentials to achieve velocity focusing [29]. Under these conditions, termed 'velocity map imaging', all products with the same velocity in the plane parallel to the detector are focused to the same point. This simple change results in a vast improvement in experimental resolution, limited in our experiments by the velocity spread of the beams. This innovation was critical to detecting the features discussed in this Report.

Figure 1 shows a raw image obtained for reactively scattered D atoms at a collision energy of  $6.1 \pm 0.6$  kcal/mol. The relative velocity vector is vertical in the plane of the figure, with the center-of-mass velocities of the reactant beams indicated. The dominant feature, quite apparent in the raw data, is the strong backscattering of the D atom relative to the incoming  $D_2$  beam, characteristic of direct rebound dynamics. However, the scattering peaks sharply near  $160^\circ$  from the  $D_2$  beam, rather than at  $180^\circ$  as would be expected for a simple rebound mechanism, and as is seen for all the backscattered contributions in the trajectory calculations. This is clearer in Figure 2A where the center-of-mass angular distribution is shown, obtained by direct inversion of the raw data. Figure 2B shows the translational energy distributions obtained from the inversion for three distinct regions of angular recoil: forward scattered,  $0-45^\circ$ , sideways scattered,  $45-135^\circ$ , and backscattered,  $135-180^\circ$ . The

forward scattered component of the distribution is distinctly faster, with an average of 9.1 kcal/mol in translation, while the backscattered component shows an average translational energy release of 7.0 kcal/mol. The sideways scattered distribution is slowest of all, showing only an average of 5.4 kcal/mol in translation. This strong coupling of translational energy release with scattering angle is expected when distinct mechanisms are operative in the different scattering directions, discussed below. This aspect of the experimental dynamics provides a further stringent test of the trajectory calculations and the quality of the potential energy surfaces.

The sharply peaked angular distribution provides insight into the nature of the potential energy surfaces involved in this reaction. We will focus our attention on near collinear O-D-D geometries, since the dominant feature in the distribution is the backscattered peak at  $160^\circ$ . Collinear approach of an  $O(^1D)$  atom to a  $D_2$  molecule results in  $\Sigma$ ,  $\Pi$  and  $\Delta$  states in the appropriate  $C_{\infty v}$  point group, which are all degenerate at long range [30]. The  $\Delta$  surface is repulsive and need not be considered at these energies. In the interaction region, the  $\Sigma$  surface is initially lower than the  $\Pi$ . The ground state products are  $OD(^2\Pi)$  and  $D(^2S)$ , so they correlate to the  $\Pi$  surface. The  $\Sigma$  surface is repulsive, correlating to electronically excited  $OD(^2\Sigma^+) + D(^2S)$ . A crossing of these surfaces must therefore occur; reactants approaching collinearly on the ground state  $\Sigma$  surface cannot yield ground state products. At energies below the threshold for formation of electronically excited  $OD(^2\Sigma^+)$ , collinear reaction is not possible and the likely result is elastic or inelastic scattering.

For geometries away from collinear, in the symmetry point group defined only by the plane of the nuclei ( $C_s$ ), the  $\Sigma$  surface becomes the ground state  $1A'$  surface, while the  $\Pi$  surface splits into  $A'$  and  $A''$  excited surfaces. The  $1A'$  ground state surface interacts strongly with the excited  $2A'$  surface: this is the conical intersection, one of the ubiquitous symmetry-induced variety. The region of the conical intersection is shown in Figure 3, roughly based on recent calculations by Dobbyn and Knowles [31]. The surfaces form a pair of inverted cones when viewed as a function of OD-D distance and O-D-D angle  $\gamma$ . Reactants approaching on the ground state  $1A'$  surface may proceed adiabatically to products, skirting

the cone, so long as the angle  $\gamma$  is sufficiently far from  $180^\circ$ . For geometries near collinear, the  $1A'$  and  $2A'$  surfaces interact strongly, and nonadiabatic transitions may occur between them. However, for strictly collinear geometries, the reaction must proceed 'diabatically' as states of different symmetry species are not coupled. The manifestation of this intersection is very clear in the scattering distribution. The strong peak at  $160^\circ$  must arise from flux on the ground state surface; reactant flux on either the  $2A'$  or  $1A''$  excited surfaces will correlate directly to products for collinear geometries, so that the backscattering from these surfaces is expected to peak at  $180^\circ$ . The observed 'V' scattering distribution represents a mapping of the likelihood of abstraction on the ground state surface onto the accessibility to the product space determined by the conical intersection. The decrease in the direct backscattered distribution is thus the shadow of the conical intersection itself. However, the details of the surfaces are more subtle than this simple picture would convey. The conical intersection occurs in the exit channel (in the region of increasing OD-D distance), and there is considerable opportunity for interaction between the  $1A'$  and  $2A'$  surfaces in the entrance channel. In addition, the collinear reaction represents a likely occasion for quantum mechanical interferences between flux on the various surfaces, yielding possible oscillations in the angular distributions and a clear potential role for the geometric phase. Future theoretical studies will be necessary to investigate these phenomena in detail.

The results have several immediate implications. The dominant source of the backscattering, even at this relatively high collision energy, is apparently from the ground state as discussed above, although small contributions from the excited  $1A''$  and  $2A'$  surfaces may also be present. For this to be the case, a dip in the backscattered reaction probability should be present even at lower collision energies, where excited states are not believed to contribute at all. In fact, some indication of this was observed in previous work in Berkeley using a 'conventional' crossed beam apparatus at a collision energy as low as 2.3 kcal/mol [20]. This is also consistent with the integral cross section measurements reported by Liu and coworkers [19] and well reproduced in the trajectory calculations of Schatz et al. [24]. The energy dependence seems to show three components: one is strongly quenched with increas-

ing collision energy as expected for the insertion mechanism involving long-range attraction. A second component appears to involve the ground state as well, but varies only slowly with collision energy. This is precisely what would be expected for collinear abstraction from the ground state. The third contribution is from excited states, for reaction above 2 kcal/mol. However, even for reaction at 6 kcal/mol these are relatively minor contributions. The fact that the trajectory calculations have never reproduced the pronounced dip in the backscattered component, and have not shown the enhancement in the forward scattering that occurs at lower collision energy, clearly shows that a more rigorous treatment is necessary. Our results call attention to the fact that, although the collinear geometry is a limiting case, since the abstraction mechanism favors reaction from such a limiting geometry, essential consequences of the symmetry must not be neglected. Although it has long been suspected that some contribution from the excited states must be considered for accurate treatment of this system at higher energies, for collinear geometries the very identity of the ground and excited states are mixed, so that treatment of the abstraction aspect of this reaction calls for a more rigorous theoretical approach.

*Notes:* For the experiment described herein, the molecular beams were configured in a counterpropagating geometry. The O(<sup>1</sup>D) beam was generated by photolyzing O<sub>3</sub> seeded in He (5% at 1 atm backing pressure), using the output of a KrF excimer laser (248 nm), at the nozzle of a piezoelectric pulsed valve. After the beam was collimated by a skimmer it was chopped by means of a rotating slotted wheel (200 Hz, 1 mm slot width), to generate a short rectangular pulse (7.5 μs) of O(<sup>1</sup>D). The oxygen atom beam velocity and spread were monitored using either (2+1) resonance-enhanced multiphoton ionization (REMPI) of O(<sup>1</sup>D) at 205nm, or conveniently using vacuum-ultraviolet (VUV) photoionization of the O<sub>2</sub> co-photofragment (using the same light used to probe the reactively scattered D atom product.) By changing the excimer laser delay relative to the chopper and probe laser, the velocity of the oxygen atom beam could be changed continuously between 1650 to 2250 m/s. Neat D<sub>2</sub> at 2 atm backing pressure was expanded through another pulsed valve and the beams were allowed to interact on the axis of the velocity focusing time-of-flight mass spectrometer. The resultant D atom was probed by using the (1+1) REMPI. The VUV Lyman-α light was generated by difference frequency mixing of ultraviolet (UV) and infrared (IR) light in krypton, phase matched with argon. The UV light (212.5 nm) was generated by doubling the output of a seeded Nd-YAG pumped dye laser operating at 637.5 nm in β-barium borate (BBO), then mixing the resulting UV light with the dye fundamental in a second BBO crystal. Infrared light around 840 nm was generated using a second Nd-YAG pumped dye laser, and the two beams were collimated using a dichroic mirror and focused into the rare gas cell. The resultant VUV output was focused into the interaction region of the molecular beams using a MgF<sub>2</sub> lens. The D<sup>+</sup> ions were accelerated towards a 40mm diameter dual microchannel plate (MCP) detector coupled to a fast phosphor screen and imaged on a fast scan charge coupled device (CCD) camera connected to an integrating video averager (Data Design AC101/I). Images were accumulated by scanning across the Doppler profile of the D atom, since the line width of the laser light was narrower than the Doppler spread. The recorded image is actually a 2-dimensional (2-D) projection of the nascent 3-dimensional (3-D) velocity distribution, but established tomographic techniques allow reconstruction of

the 3-D distribution. Typical accumulation time for a single collision energy was about 90 minutes. A background image obtained with the excimer off was subtracted from the data image, but this represented a minor correction.

## REFERENCES

- [1] G. Herzberg, *Molecular Structure and Molecular Spectra Vol. III* (Krieger, Malabar, Florida, 1991).
- [2] D. Yarkony, *J. Phys. Chem.* **100**, 18612 (1996).
- [3] J. C. Tully, *Int. J. Quantum. Chem.* **S25**, 299 (1991).
- [4] G. Herzberg and H. C. Longuet-Higgins, *Disc. Far. Soc.* **35**, 77 (1963).
- [5] C. Mead, *Rev. Mod. Phys.* **64**, 51 (1992).
- [6] P. W. Kash, G. C. G. Waschewsky, R. E. Morse, L. J. Butler, and M. M. Francl, *J. Chem. Phys.* **100**, 3463 (1994).
- [7] R. Feng, X. S. Zheng, and G. E. Hall, *J. Phys. Chem. A* **101**, 2541 (1997).
- [8] R. Baer, D. Charutz, R. Kosloff, and M. Baer, *J. Chem. Phys.* **105**, 9141 (1996).
- [9] Y.-S. Wu and A. Kuppermann, *Chem. Phys. Lett.* **201**, 93 (1993).
- [10] D. Neuhasuer, R. S. Judson, D. J. Kouri, D. E. Adelman, N. E. Shafer, D. A. V. Kliner, and R. N. Zare, *Science* **257**, 519 (1992).
- [11] E. Wrede, L. Schnieder, K. Welge, F. J. Aoiz, L. Banares, V. J. Herrero, B. Martinez-Haya, and V. S. Rabanos, *J. Chem. Phys.* **106**, 7862 (1997).
- [12] R. Buss, P. Casavecchia, T. Hirooka, H. Sibener, and Y. Lee, *Chem. Phys. Lett.* **82**, 386 (1981).
- [13] R. Schinke and W. A. Lester, *J. Chem. Phys.* **72**, 3754 (1980).
- [14] J. N. Murrell and S. Carter, *J. Phys. Chem.* **88**, 4887 (1984).
- [15] P. M. Aker, J. J. Sloan, and J. S. Wright, *Chem. Phys.* **110**, 275 (1986).
- [16] T. Ho, T. Hollebeek, H. Rabitz, L. Harding, and G. Schatz, *J. Chem. Phys.* **105**, 10472

- (1996).
- [17] A. J. A. and F. J. Aoiz, M. Brouard, and J. P. Simons, *Chem. Phys. Lett.* **256**, 561 (1996).
- [18] D. Che and K. Liu, *J. Chem. Phys.* **103**, 164 (1995).
- [19] Y. Hsu, J. Wang, and K. Liu, *J. Chem. Phys.* (in press, 1997).
- [20] T. T. Miao, Ph.D. Thesis, University of California, Berkeley, 1995.
- [21] Y. Hsu and K. Liu, *J. Chem. Phys.* (1997).
- [22] P. Cassavechia, Personal communication (1997).
- [23] P. J. Kuntz, B. I. Niefer, and J. J. Sloan, *Chem. Phys.* **151**, 77 (1991).
- [24] G. Schatz, A. Papaioannou, L. Pederson, L. R. Harding, T. Hollebeek, T. Ho, and H. Rabitz, *J. Chem. Phys.* (in press) (1997).
- [25] D. W. Chandler and P. L. Houston, *J. Chem. Phys.* **87**, 1445 (1987).
- [26] A. G. Suits, L. J. Bontuyan, P. L. Houston, and B. J. Whitaker, *J. Chem. Phys.* **96**, 8618 (1992).
- [27] T. A. Kitsopoulos, D. P. Baldwin, M. A. Buntine, R. N. Zare, and D. W. Chandler, *Science* **260**, 1605 (1993).
- [28] M. Ahmed, D. Blunt, D. Chen, and A. G. Suits, *J. Chem. Phys.* **106**, 7617 (1997).
- [29] A. T. J. B. Eppink and D. H. Parker, *Rev. Sci. Instrum.* (in press) (1997).
- [30] S. Walch and L. Harding, *J. Chem. Phys.* **88**, 7653 (1988).
- [31] A. J. Dobbyn and P. J. Knowles, *Mol. Phys.* (in press) (1997).

### ACKNOWLEDGMENTS

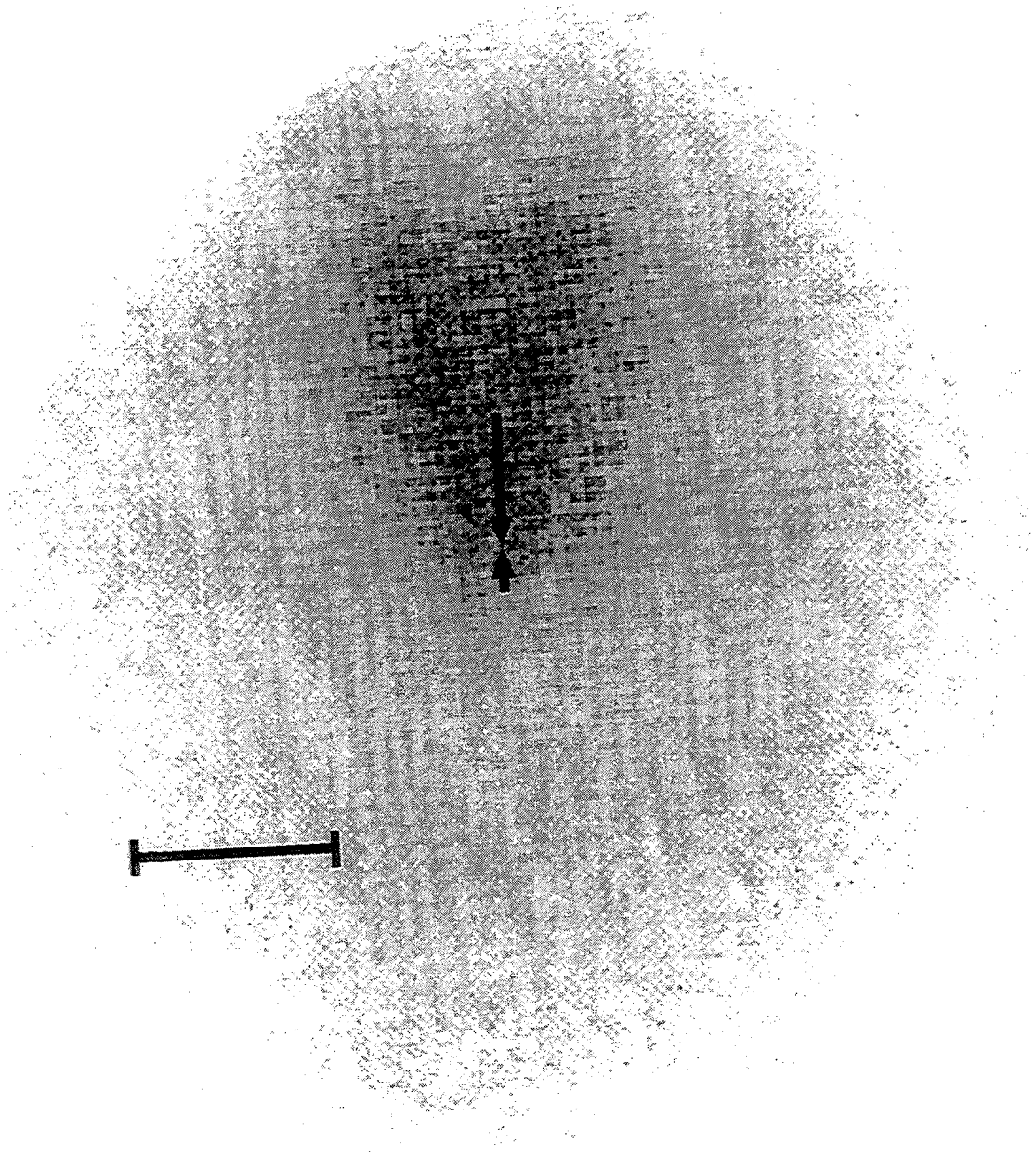
The authors gratefully acknowledge G. Schatz and P. Cassavechia for valuable discussions and comments on the manuscript, and K. Liu, G. Schatz, D. Parker, P. Cassavechia and P. J. Knowles for providing preprints of their most recent work. AGS would like to thank D. Chandler and the Sandia Combustion Research Facility for hosting a recent workshop on imaging methods at which the velocity mapping technique was discussed. This work was supported by the Director, Office of Energy Research, Office of Basic Energy Sciences, Chemical Sciences Division of the U. S. Department of Energy under contract No. DE-ACO3-76SF00098.

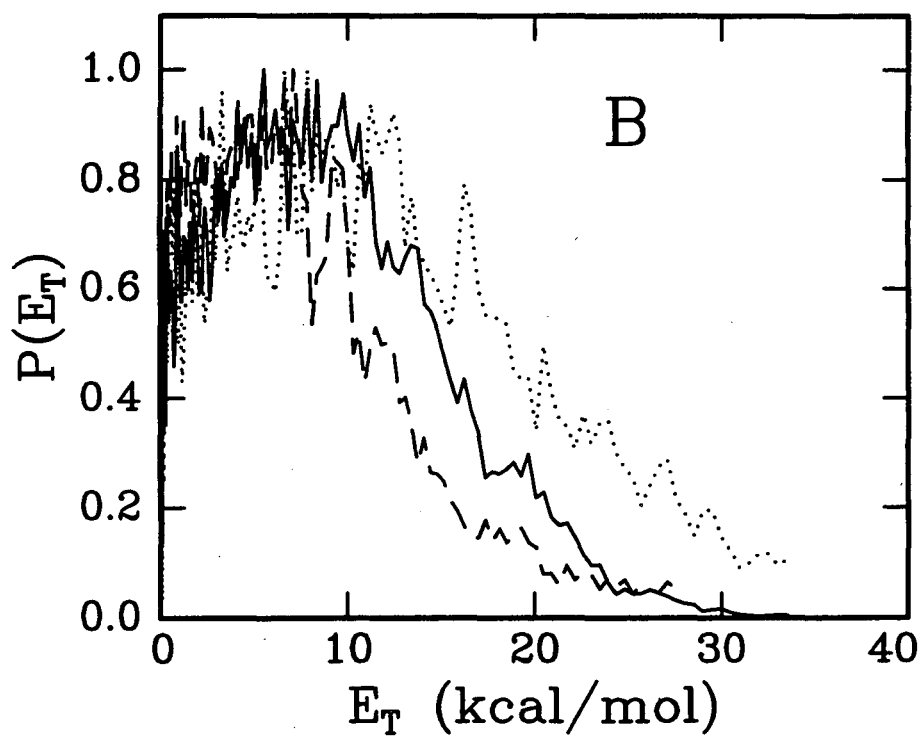
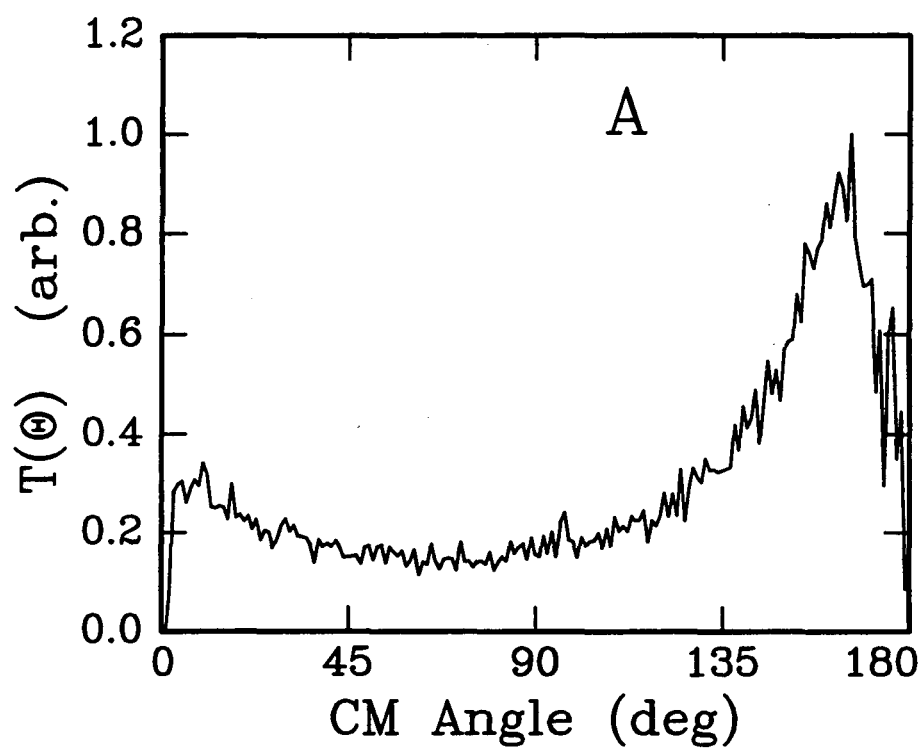
## FIGURES

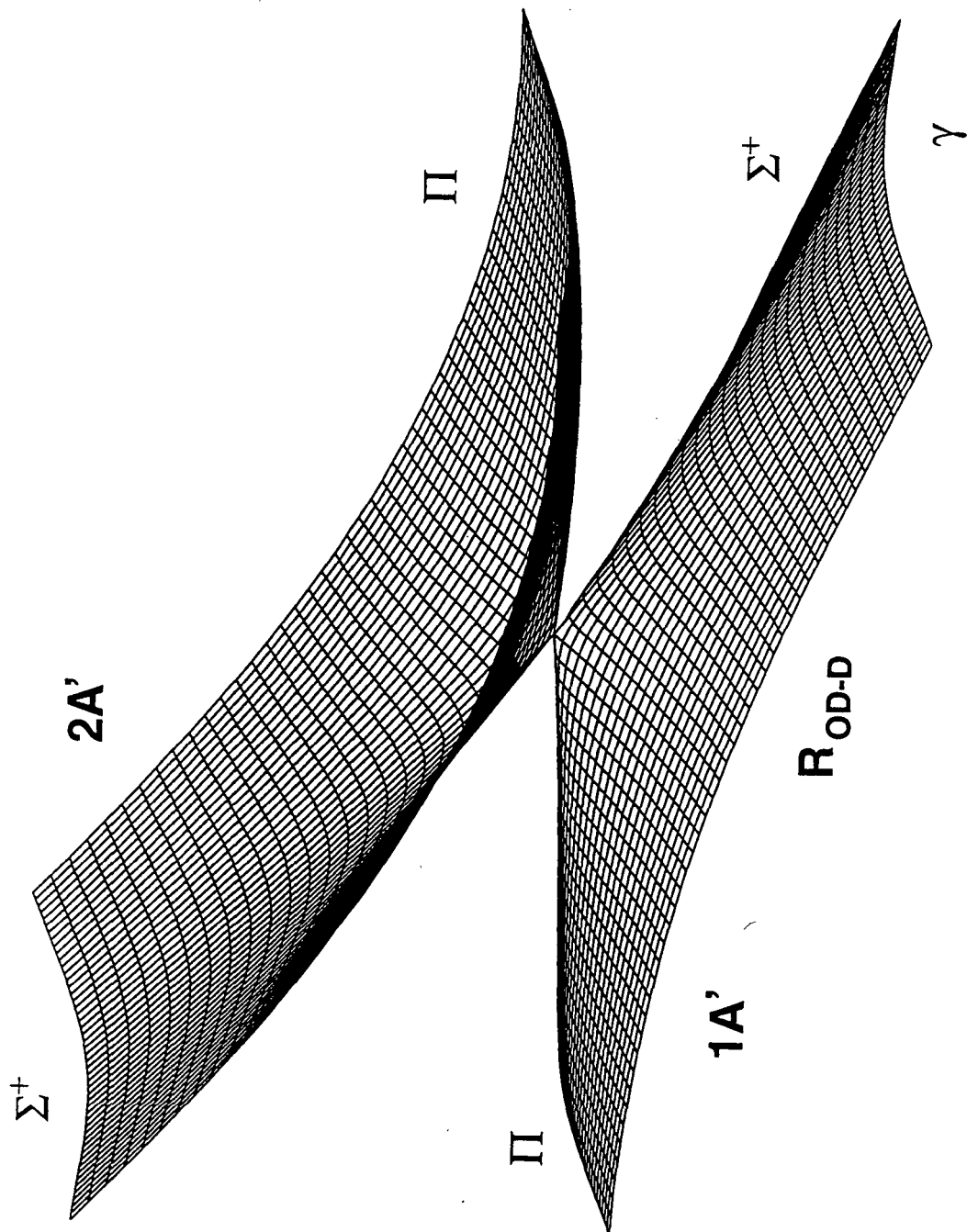
Fig. 1 Image of D atoms from reaction  $O(^1D) + D_2$  at a collision energy of 6.1 kcal/mol. The scale bar represents 4 km/s and the arrows show the relative velocities of the beams in the center-of-mass frame. The short arrow corresponds to the  $O(^1D)$  beam while the long arrow represents the  $D_2$  beam.

Fig. 2 A. Center of mass angular distribution obtained from the image in Fig. 1. The direction of the  $D_2$  and  $O(^1D)$  beams correspond to  $0^\circ$  and  $180^\circ$ , respectively. B. Translational energy distributions obtained from the image. Dotted line,  $0-45^\circ$ , dot-dash,  $45-135^\circ$ , solid,  $135-180^\circ$ .

Fig. 3 Illustration of the region of conical intersection. The range of  $\gamma$  is  $180^\circ \pm 5^\circ$ . The region of increasing OD-D distance leading to products is to the left of the figure. The labels  $\Sigma$  and  $\Pi$  refer to the centerline of the surfaces, for  $\gamma=180^\circ$ .







**ERNEST ORLANDO LAWRENCE BERKELEY NATIONAL LABORATORY  
ONE CYCLOTRON ROAD | BERKELEY, CALIFORNIA 94720**